JBC Papers in Press. Published on August 10, 2007 as Manuscript M703259200
The latest version is at http://www.jbc.org/cgi/doi/10.1074/jbc.M703259200

INHIBITION OF SKELETAL MUSCLE ClC-1 CHLORIDE CHANNELS BY LOW INTRACELLULAR pH AND ATP

Brett Bennetts, Michael W. Parker & Brett A. Cromer*
From St. Vincent's Institute, Fitzroy, Vic. 3065, Australia, *BAC current address: Howard Florey Institute, University of Melbourne, Vic. 3010 Australia
Running head: ClC-1 inhibition by low pH and ATP

Address correspondence to: Brett A. Cromer - brett.cromer@florey.edu.au, Howard Florey Institute, University of Melbourne, Vic. 3010 Australia. Tel:+61 3 8344 1648, Fax:+61 3 9347 0466,
or Brett Bennetts - bbennetts@svi.edu.au, St. Vincent's Institute, 9 Princes St., Fitzroy, Victoria 3065, Australia. Tel:+61 3 9288 2480, Fax:+61 3 9416 2676,

Skeletal muscle acidosis during exercise has long been thought to be a cause of fatigue but recent studies have shown that acidosis maintains muscle excitability and opposes fatigue by decreasing the sarcolemmal chloride conductance. ClC-1 is the primary sarcolemmal chloride channel and has a clear role in controlling muscle excitability but recombinant ClC-1 has been reported to be activated by acidosis. Following our recent finding that intracellular ATP inhibits ClC-1, we investigated here the interaction between pH and ATP regulation of ClC-1. We found that in the absence of ATP, intracellular acidosis from pH 7.2 to 6.2 inhibited ClC-1 slightly by shifting the voltage dependence of common gating to more positive potentials, similar to the effect of ATP. Importantly, the effects of ATP and acidosis were cooperative, such that ATP greatly potentiated the effect of acidosis. Adenosine had a similar effect to ATP at pH 7.2 but acidosis did not potentiate this effect, indicating that the phosphates of ATP are important for this cooperativity, possibly due to electrostatic interactions with protonatable residues of ClC-1. A protonatable residue identified by molecular modelling, His847, was found to be critical for both pH and ATP modulation and may be involved in such electrostatic interactions. These findings are now consistent with, and provide a molecular explanation for, acidosis opposing fatigue by decreasing the chloride conductance of skeletal muscle via inhibition of ClC-1. The modulation of ClC-1 by ATP is a key component of this molecular mechanism.

Action potentials of skeletal-muscle membranes occur due to a depolarisation induced transient inward Na^+ current through channels that rapidly inactivate at depolarised potentials. As the equilibrium potentials for both K^+ and Cl^- are close to the resting membrane potential, K^+ and Cl^- currents oppose the depolarising contribution of inward Na^+ currents. Voltage-gated K^+ channels that activate immediately after Na^+ channels are important for returning the membrane potential to resting levels after an action potential. During vigorous muscle activity, however, extracellular K^+ can accumulate, leading to membrane depolarisation and probably chronic inactivation of Na^+ channels (1,2), in turn leading to reduced inward Na^+ current, a factor thought to contribute to muscle fatigue. At rest approximately 80% of the total membrane conductance is carried by Cl^- (3), the vast majority through weakly voltage-dependent ClC-1 chloride channels (4) as demonstrated by mice deficient in ClC-1 whose muscle chloride conductance (G_{Cl}) is reduced to less than 10% of that of wild-type mice (5). In order for action-potential initiation and propagation to occur the magnitude of Na^+ current must be great enough to overcome electrical shunting through open ClC-1 channels and depolarise the muscle membrane. A reduction of G_{Cl} due to ClC-1 inhibition decreases the amount of inward current required to depolarise the membrane, i.e. increases the excitability of the membrane. The importance of this function of ClC-1 is underlined by the genetic disease myotonia, in which loss-of-function mutations of ClC-1 lead to skeletal muscle hyper-excitability (6). Many myotonia-causing mutations shift ClC-1 voltage-dependence to more positive potentials resulting in channel inhibition across the physiological voltage range (7).

Working muscle becomes acidified due to lactic acid accumulation during moderate to high intensity activity (8). Acidification has been shown to result in recovery of muscle excitability and force when these have decreased due to elevated

extracellular [K^+] (9). More recent studies have shown that increased excitability at low intracellular pH (pH_i) is due to reduced chloride conductance of the muscle membrane (10,11). Low pH has long been known to reduce G_{Cl} in muscle membranes (12,13), but previous studies of the pH sensitivity of recombinantly expressed ClC-1 have failed to reconcile the reduction of G_{Cl} of the membrane with a molecular mechanism acting directly on ClC-1. In patch-clamp studies of heterologously expressed ClC-1 low pH_i activated the channel by shifting voltage-dependence of gating to more negative potentials (14-16). If acidosis caused similar activation of ClC-1 in the muscle membrane, this would tend to increase G_{Cl} and decrease membrane excitability, contrary to what is observed. Given that ClC-1 is responsible for the vast majority of the sarcolemmal G_{Cl}, this contradiction is unlikely to be explained by decreased activity of sarcolemmal chloride channels other than ClC-1. Rather it appears likely that there is some aspect of the *in vivo* pH effects on ClC-1 that are not recapitulated when ClC-1 is recombinantly expressed.

ClC-1 is a skeletal muscle-specific member of the ClC family of chloride channels and transporters. All eukaryotic members of this family comprise a large membrane-embedded domain followed by two cytoplasmic cystathionine β-synthase related (CBS) domains. The prototypical, and best studied, channel in this family is ClC-0 from the electric organ of *Torpedo* electric rays. Based initially on the characterisics of ClC-0 single-channel records (17) and supported by the structures of bacterial ClC homologs (18), there is good evidence that ClC proteins function as homo-dimers in which each monomer contains a separate ion-conducting pore. Single channel records of both ClC-0 (17) and ClC-1 (19) show two distinct forms of gating, rapid "protopore gating", that independently opens or closes individual pores within a dimer, and a slower "common gating" process that opens or closes both pores simultaneously. For ClC-1, the two gating mechanisms have relatively similar kinetics at negative potentials but can be kinetically separated in whole cell currents with a short pulse to very positive potentials, selectively opening the protopore gate (14). Protopore gating appears to involve very minor changes in protein structure, primarily movement of a conserved glutamate sidechain at the extracellular channel mouth (20). In contrast, common gating appears to entail major conformational changes (21,22), involving the dimer interface of the membrane domain (23) as well as the cytoplasmic CBS domains (24,25).

Previously we have shown that ATP inhibits ClC-1 by shifting the voltage-dependence of common gating to more positive potentials, a process mediated by the intracellular CBS domains (24). We postulated that the physiological relevance of ATP modulation of ClC-1 may be to protect cells from metabolic exhaustion by increasing G_{Cl} and decreasing muscle excitability when ClC-1 inhibition is relieved due to ATP depletion during intense activity, or ischemia (24). Here we show that in the presence of ATP, intracellular acidosis inhibits ClC-1 by enhancing both ATP sensitivity and the maximal effect of ATP on common gating, and that His847 in CBS domain 2 is a key residue in this process. These findings identify a molecular mechanism for the modulation of recombinant ClC-1 by acidosis that, in the presence of physiological intracellular concentrations of ATP, is consistent with the decreased G_{Cl} and increased excitability seen with acidosis in skeletal muscle. These findings also indicate that the primary physiological significance of ATP modulation of ClC-1 may be in maintaining excitability and opposing fatigue by potentiating the inhibitory effect of acidosis on ClC-1.

Experimental Procedures

Channel expression and site-directed mutagenesis- Human *ClCN1* was expressed using a pCIneo (Promega) mammalian expression vector, as detailed previously (21,26). Human embryonic kidney (HEK293T) cells (American Type Culture Collection, Rockville, MD, USA) were transiently transfected with a mixture of the *ClCN1* construct and pEGFP-N1 (Clontech) reporter plasmid at a molar ratio of 3:1 using Fugene 6 (Roche), according to the manufacturer's specifications. Transfected cells were later identified by reporter-plasmid driven expression of the green fluorescent protein. Mutations were introduced into *ClCN1* using the Quickchange (Stratagene) mutagenesis technique and confirmed by DNA sequencing.

Electrophysiology- Patch-clamp experiments were conducted at room temperature (23 ± 1 °C) in the whole-cell configuration using an Axopatch 200B patch-clamp amplifier (Axon Instruments, Foster City, CA, USA) and associated standard equipment. Cells were continuously superfused with bath solution containing (mM): NaCl, 140; CsCl, 4; $CaCl_2$, 2; $MgCl_2$, 2; HEPES, 10; adjusted to pH 7.4 with NaOH. The standard pipette solution contained (mM): CsCl, 40; Caesium glutamate, 80; EGTA-Na, 10; HEPES, 10; adjusted to pH 7.2 with NaOH. For low pH internal solutions, 10 mM MES was substituted for HEPES and the pH adjusted with NaOH. ATP was added to the pipette solution as a magnesium salt at a concentration of 5 mM. Adenosine was added to the pipette solution at a concentration of 5 mM. The pH was readjusted with NaOH after addition of ATP or adenosine. Aliquots were stored at -20 °C and diluted on the day of the experiment.

Patch pipettes were pulled from borosilicate glass, and typically had resistance of 1-2 MΩ when filled with the above pipette solution. Series resistance did not exceed 4 MΩ and was 85-95 % compensated. After rupturing the cell membrane and achieving the whole-cell configuration, no less than 5 minutes was allowed for the pipette solution to equilibrate with the intracellular solution before current recordings were made. Currents obtained at a sampling frequency of 10 kHz were filtered at 5 kHz, and collected using Axograph 4.9 (Axon Instruments, Foster City, CA, USA) software. Applied membrane potentials were adjusted for junction potentials calculated using JPCalc (27).

Voltage dependent channel activity was measured by applying a voltage test pulse, stepping in successive sweeps from –140 to +100 mV in 20 mV steps for a duration of 100-800 ms. This was followed by a 75 ms tail pulse at a set 100 mV. The instantaneous current amplitude at the start of the tail pulse was used as a measure of the open probability at the end of the test pulse. To measure the open probability of the common gate only, the protopore gate was fully opened by a 400 μs pulse to +170 mV between the test pulse and the tail pulse (14). The membrane was clamped to –30 mV for a period of 2 s between each sweep.

Data analysis- Data were analyzed using Axograph 4.9 (Axon Instruments, Foster City, CA, USA) and GraphPad Prism 4.0 (GraphPad software, San Diego, CA, USA) software. The channel open probability at the end of the test pulse, as a function of test pulse voltage, was determined by measuring the instantaneous current at the start of the tail pulse. This instantaneous current was determined by fitting current relaxations during the –100 mV tail pulse with an equation of the form

$$I(t) = A_1 \exp\left(t/\tau_1\right) + A_2 \exp\left(t/\tau_2\right) + C \qquad (1)$$

where I is the whole-cell current, t is time, τ_1 and τ_2 are the time constants of the fast and slow components of current relaxation, respectively, and A_1, A_2 and C are the amplitudes of the fast, slow and steady-state components of the current, respectively. Instantaneous current amplitudes at the start of the –100 mV pulse ($I(0)$) were determined by extrapolation of this function. To obtain the voltage dependence of the apparent channel open-probability (P_o), normalised instantaneous current amplitudes were fit with a modified Boltzmann distribution of the form

$$P_o(V) = P_{\min} + \frac{1 - P_{\min}}{1 + \exp\left(\left(V_{1/2} - V\right)/k\right)} \qquad (2)$$

where $P_{\min}$ is an offset, or a minimal open probability at very negative potentials, V is the membrane potential, $V_{1/2}$ is the half-maximal activation potential, and k is the slope factor. To determine the voltage dependence of the slow, common gate that acts simultaneously on both protopores of the channel a 400 μs pulse to +170mV was inserted before the –100 mV tail pulse, to maximally activate the fast, protopore gates. Instantaneous tail-current amplitudes determined as described above were fit with equation (2) to yield $P_o(V)$ for the common gate. Open probability of the protopore gate was determined by dividing the apparent channel open probability by the open probability of the common gate. This data was fit with equation (2) to yield $P_o(V)$ curves for the protopore.

In order to determine the time course of current relaxations, activating currents were recorded for 500 ms at voltages from 0 to 100 mV in 20 mV increments directly after a 200 ms pulse to –140 mV to deactivate channels. Deactivating currents

were recorded during 500 ms pulses between –140 and –40 mV in 20 mV increments directly after a 200 ms pulse to 100 mV to maximally activate current. Current activation was typically bi-exponential with time constants in the order of milliseconds and 10's of milliseconds (not shown). Deactivating currents were fit with two exponentials using eq. (1), where the fast (τ_1) and slow (τ_2) time constants are thought to correspond to protopore and common gating processes respectively (14). Detailed characterisation of ClC-1 gating transitions has indicated that at positive potentials the exponential component due to protopore gating is likely to be too fast to resolve in macroscopic current activation (14), so only the single exponential of common gating should be resolved. There were indications, however, of two exponentials in the time course of current activation, consistent with earlier reports (23). As the two components could not be assigned to particular gating transitions, they were assumed to both contribute to the slow gating process and to simplify subsequent calculations of rate constants, the time course was approximated with a single-exponential function (23) of the form,

$$I(t) = A\exp\left(t/\tau\right) + C \qquad (3)$$

where τ is assumed to correspond to common gating. The apparent opening (α) and closing (β) rate constants of the common gate were calculated from the time constants for current deactivation (τ_2, from eq. (1)) and activation (τ, from eq. (3)) and the open probability P_o using the equations (28),

$$\alpha = P_o/\tau \qquad (4a)$$

$$\beta = (1 - P_o)/\tau \qquad (4b)$$

Unless otherwise labelled all data, except raw current traces, are presented as the mean ± SEM of recordings from three or more cells.

RESULTS

Dependence of ClC-1 gating on intracellular pH- In experiments with isolated rat diaphragm muscle fibres, Palade and Barchi (1997) noted that low pH reduced chloride conductance of the muscle membrane over a time course of 15-20 minutes, with the prolonged equilibration time potentially indicating that the titratable groups are present inside the cell. In support of this notion, experiments with mechanically skinned extensor digitorum longus muscle fibres from rat demonstrated that intracellular acidification leads to decreased chloride permeability of the t-tubular system (11).

With this in mind we re-examined the dependence of ClC-1 gating on intracellular pH by using whole-cell voltage clamp experiments to measure the channel activity of recombinant human ClC-1 expressed in HEK-293T cells. The intracellular pH was controlled by the buffered pH of the pipette solution. To ensure that the intracellular milieu had equilibrated with the pipette solution, current recordings were only made more than five minutes after achieving whole-cell patch configuration by rupturing the membrane across the pipette tip. We cannot be sure of the precise intracellular pH but, given the buffering capacity and relatively massive volume of the pipette solution, we assume that it matches that of the pipette solution. Consequently, we have not attempted to change the pH of the pipette solution during an experiment so each cell is tested at only one internal pH. Measurement of ClC-1 currents in excised inside-out membrane patches would facilitate the ready exchange of the effective intracellular milieu but we were unable to obtain sufficiently stable ClC-1 currents in this patch configuration.

Previous electrophysiological studies of ClC-1 dependence on intracellular pH have used relatively short, 100-200 ms, voltage pulses in order to drive the gating into steady-state (14,15,29). Because the kinetics of ClC-1 macroscopic current relaxations are slowed at low pH_i (14,15,29) we explored the use of longer voltage test pulses to ensure that the slow component of current relaxation, corresponding to common gating (14), reached steady-state before measuring open probability with a set-voltage tail pulse. With the pipette (intracellular) solution at pH 6.2, we examined the effect on ClC-1 gating of progressively longer voltage test pulses, from 100-800 ms (Fig. 1A). To restrict our measurements to the common gate only, a 400 μs pulse to +170 mV was inserted at the end of the test pulse prior to the -100 mV tail pulse (Fig. 1A). Insertion of a short

pulse such as this has been shown previously to completely open the protopore gate but is too short to have any significant effect on the common gate (14). Consequently, the tail current immediately after this short pulse gives a measure of the open probability of the common gate alone. As the open probability overall is the product of that of the two gates, the open probability of the protopore gate can be determined by dividing the open probability overall by that of the common gate. Sample traces of the currents in response to different length test pulses (shown in Fig. 1B, with sweeps at different test pulse voltages overlaid), clearly demonstrate that currents did not reached steady until the test pulse was longer that 400 ms. The instantaneous current peak at the start of the tail pulse, which measures open probability, also clearly changes with the length of test pulse, although the details of this are not clear until it is normalised and plotted against test pulse voltage (Fig. 1C). The longer test pulses clearly shifted the apparent voltage dependence of common gating to more positive potentials (Fig. 1C), emphasizing the importance of applying pulses of sufficient length to allow gating to reach equilibrium.

Visual inspection and fitting of exponentials to gating relaxations (data not shown) indicated that gating had essentially equilibrated by the end of an 800 ms voltage pulse. To ensure that chloride currents during these long voltage pulses had not significantly shifted the chloride equilibrium, we used current-clamp mode to measure the voltage at which there was zero current. This did not change immediately before and after the 800 ms voltage (results not shown), indicating that these longer pulses did not significantly affect chloride equilibrium, consistent with the work of others using similar voltage pulses (23). Consequently we have used 800 ms voltage pulses throughout the remainder of this study.

We next used these voltage pulse protocols to examine the effect of varying intracellular pH (Fig. 2A) on the voltage dependence of ClC-1 channel open probability. We measured both the overall open probability, by omitting the 400 μs pulse to +170 mV at the end of test pulse, and the common gate open probability, by including this pulse. We could then calculate open probability of the protore gate by dividing the overall apparent open probability by that for the common gate. The voltage dependence of the overall apparent open probability had an unusual bi-phasic dependence on intracellular pH (pH_i), such that it was most negative at pH 7.2 and was shifted to more positive voltages at both higher and lower pH (Fig. 2B). When the contributions of common (Fig. 2C) and protopore (Fig. 2C) gating to the overall channel open probability were dissected it became clear that this biphasic pH dependence arises from the effect of pH on common gating. With a minimum at approximately pH 7.2, changing pH_i in either direction shifted the voltage dependence of common gating to more positive potentials (Fig. 2C). At the same time, decreasing pH_i below 7.2 reduced the minimum value of the gating curve, P_{min}^{common}. In contrast, and as previously reported (14), decreasing pH_i below 7.2 shifted the voltage dependence of protopore gating to slightly more negative potentials and the minimum value of the gating curve was increased (Fig. 2D). Overall, when both gating mechanisms are taken into account, a decrease in pH from 7.2 to 6.2 reduced the open probability of ClC-1 across the range of physiologically relevant membrane potentials, consistent with the reduced skeletal muscle sarcolemmal chloride-conductance observed with acidosis (10-13).

The effects of intracellular ATP and protons on ClC-1 common gating are synergistic- Previously we have shown that intracellular ATP shifts the voltage dependence of ClC-1 common gating to more positive potentials (24), in a similar manner to the effect of acidosis described above. As acidosis and ATP depletion can both occur in working skeletal muscle, we were interested to examine the interaction of these two modulatory effects on ClC-1. Consequently, we compared the effects on ClC-1 gating of acidosis and ATP, independently and in combination. Consistent with our previous finding that ATP had no effect on protopore gating of ClC-1 (24), we found that ATP had no effect on the pH dependence of protopore gating (data not shown). The effects of protons and ATP on the voltage dependence of common gating were found to be synergistic, with the two combined causing a shift to more positive potentials that was greater than the additive effects of each individually (Fig. 3A and 3B). Indeed, the voltage dependence of common gating was shifted to such an extent that P_o curves showed no obvious saturation at +100 mV, the maximum positive voltage for which we could make stable recordings, leading to increased uncertainties when

fitting these data to a Boltzmann distribution and, most importantly, in the estimate of $V_{1/2}$. The best fit of the P_o data for 1 mM ATP at pH 6.2 (Fig. 3B) gives a $V_{1/2}$ of +71 mV but may be much greater or slightly less than this value without significantly reducing the goodness of fit. It is unlikely, however that the $V_{1/2}$ is markedly less than +71 mV as this should show up as a clear inflection point in the data. The shift in the $V_{1/2}$ ($\Delta V_{1/2}$) due to a change in pH from 7.2 to 6.2 was increased approximately 3-fold or more by the presence of saturating ATP. Similarly, the $\Delta V_{1/2}$ due to saturating intracellular ATP was increased approximately 2-fold or more by intracellular acidosis from pH_i 7.2 to 6.2 (Fig. 3C). Furthermore, a shift in pH from 7.2 to 6.2 seems to increase the apparent affinity for ATP (Fig. 3C). Certainly, lowering the pH increases the $\Delta V_{1/2}$ caused by low concentrations of ATP but, because of the uncertainty in the measurement of $V_{1/2}$ in high [ATP], it is not clear whether this increase is entirely due to the larger magnitude of the effect of ATP or if it is partly due to a higher apparent affinity for ATP.

Next we measured a more complete dose-response relationship for the effect of protons on $V_{1/2}$. An effective titration was difficult to achieve, however, because of both the narrow pH range over which whole-cell currents could be measured and the relatively small effect of pH on $V_{1/2}$ in the absence of ATP. At 1 mM intracellular ATP the effect of pH on $V_{1/2}$ was great enough for a reasonable pH titration curve to be measured (Fig. 3D) but the data did not reach a clear plateau at low pH and suffers further from the uncertainty in $V_{1/2}$ estimates in this region. Also because 1mM ATP is not saturating in the higher pH range of this titration, part of the $\Delta V_{1/2}$ may be due to changes in ATP affinity. Consequently, it is not feasible to make a precise estimate of the apparent pK_a for the effect of protons on common gating, but this data does indicate that the pK_a is below 6.7 and is broadly compatible with the apparent pK_a of 5.5 obtained for whole muscle chloride conductance (13). This in vivo measurement of pK_a may be an underestimate because the pH values in this study were reported for the external solution, while the titratable group(s) are probably located on the inside of the cell membrane (13). Although the data presented above does not allow us to precisely define all the parameters of pH and ATP modulation of ClC-1 common gating, it clearly demonstrates that physiological concentrations of ATP dramatically enhance the inhibitory effect of acidosis on ClC-1, identifying a vital factor in rationalising the regulation of recombinant ClC-1 with the regulation of skeletal muscle chloride conductance *in vivo*.

The synergistic interaction between the effects of ATP and protons on common gating may be due to allosteric mechanisms or may involve direct interactions between ATP and protons at their binding sites on ClC-1, particularly electrostatic interactions between protons and the phosphates of ATP. We have shown previously that at pH_i 7.2 the effect of adenosine on common gating is very similar to that of ATP (24). If proton potentiation of the effects of ATP occurs via an allosteric mechanism, then similar potentiation of the effects of adenosine would be expected. Conversely, if proton potentiation is due to electrostatic interactions with the phosphates of ATP, then it obviously should not occur for adenosine. We found that the effect of intracellular adenosine on common gating was very similar at pH 7.2 or 6.2 (Fig. 3C), with no significant change in $\Delta V_{1/2}$ or the apparent affinity for adenosine. These data demonstrate that the proton potentiation of the effect of ATP requires the phosphates of ATP and so is more consistent with a direct electrostatic interaction than an allosteric mechanism. Furthermore these data demonstrate that proton potentiation is not due to protonation of the adenosine moiety. The pH titration for proton potentiation (Fig. 3D) is consistent with the pK_a for protonation of the γ-phosphate of ATP (30) or for protonation of a number of amino acid side-chains, particularly histidine but also possibly glutamate and aspartate. Taken together, these data support the hypothesis that the enhanced effect of ATP with acidosis is due to direct electrostatic interactions between the phosphate groups of ATP and charged residues of ClC-1, where one of these two partners becomes protonated.

Improved modelling of a putative ATP-binding site in CBS domains of ClC-1- We have presented previously (24) a model of the CBS domains of ClC-1 built by homology to related domains in inosine-monophosphate dehydrogenase (pdb entry 1ZFJ). Guided by computational docking of nucleotides to this model, we showed that His847 in CBS2 of ClC-1 is important for modulation of ClC-1 by ATP and proposed that it interacts with

the ribose moiety of ATP bound in the cleft between the two CBS domains (24). It was this hypothesized interaction that prompted us to investigate the interaction between protons and ATP in ClC-1 modulation, described above. Recent structural data for CBS domains of ClC-1 has enabled us to refine and re-evaluate our model of ClC-1 CBS domains and the mode of nucleotide binding. Firstly, Meyer and Dutzler have resolved the structure of the CBS domains of ClC-0 (31) providing strong support for many features of our ClC-1 CBS domain model, in particular the positioning of His847 and Leu848 at the mouth of the cleft between CBS-1 and -2. This structure does not, however, tell us anything about ATP binding as there were no nucleotides bound. Indeed ClC-0 appears not to bind nucleotides (31). More recently, however, Meyer and colleagues have resolved the structure of CBS domains from ClC-5 with nucleotides bound (32). ATP and AMP were resolved bound in the central cleft between the two CBS domains of ClC-5 (32) as we predicted for ClC-1 (24) but on the opposite side of the cleft to our prediction.

To investigate the implications of these structures for nucleotide binding in ClC-1, we built a new model of the CBS domains of ClC-1 by homology to the ClC-0 structure, PDB code 2D4Z (31), as ClC-0 is the closest homolog of ClC-1 with approximately 70% identical residues in the CBS regions. Although very similar to our earlier model (24), there were a number of significant changes in the new model, including a slight reorientation of the two CBS domains relative to each other and extension of the model both into the loop between CBS-1 and -2 and at the N-terminus, considerably restructuring a loop bounding the central cleft. Docking of AMP, as described previously (24), to this new model indicated that binding was feasible on either side of the central cleft (Fig. 4), with one orientation closely matching that from docking to our earlier model (24) and the other orientation closely matching that of AMP or ATP bound to CBS domains of ClC-5 (31). The latter orientation was not feasible in our earlier model due to partial occlusion of the cleft by the shorter N-terminal loop. The two orientations appear equally consistent with our experimental evidence showing the importance of His847 and Leu848 for modulation of ClC-1 by ATP (24), as they both have similar interactions with these centrally located residues but from opposite sides (Fig. 4). Interestingly, a very recently resolved structure of CBS domains from AMP-activated protein kinase (33) reveals nucleotides bound in a similar manner to that seen in ClC-5, despite minimal sequence similarity. Such similarities in distantly related proteins support a conserved mode of nucleotide binding by CBS domains, but this remains to be specifically confirmed for ClC-1.

The role of histidine residues in CBS2- Next we investigated the hypothesis that histidine side-chains, having the most appropriate pK_a, are likely contenders for the proton acceptors mediating the effect of pH on ATP modulation of ClC-1 common gating. Previously we used molecular modelling to identify His847 in CBS2 of ClC-1 for mutational studies and showed it is a critical residue for ATP modulation of ClC-1 (24). Based on this original model, we proposed that this residue may interact with the ribose moiety of bound ATP (24), but it also may be in appropriate proximity to interact electrostatically, when protonated, with the phosphates of bound ATP. In our new model, with an alternative ATP binding position (Fig. 4) this electrostatic interaction remains feasible. To test this possible interaction, we examined the pH and ATP sensitivity of mutants of H847 (Fig. 5). Mutation of His847 to alanine (His847Ala) essentially abolished the effect of lowering pH_i on the voltage dependence of common gating although there was a slight increase in the minimum open probability when pH_i was increased to 7.9 (Fig. 5B, Table 1). The His847Ala mutation also essentially abolished the effect of ATP on the $V_{1/2}$ of common gating at pH 7.2, as shown previously (24), and reduced the effect of ATP by more than 80% at pH 6.2 (Fig. 5B, Table 1). These results demonstrate that His847 is a critical residue for the effects of both protons and ATP on common gating by, consistent with it being involved in the binding of both ligands. As the independent effects of either protons or ATP are eliminated by the His847Ala mutation, no specific conclusions can be reached about the role of His847 in mediating the synergistic effects of both together, in particular via electrostatic interaction between protonated His847 and the phosphates of ATP.

To further probe the role of His847 protonation, we sought to replicate the electrostatic effect of protonation by substituting His847 with a more basic arginine residue that would be fully

protonated across the pH range tested. Similar to His847Ala, the His847Arg mutation effectively eliminated the effect of ATP on common gating at pH 7.2 and greatly reduced its effect at pH 6.2 (Fig. 5C, Table 1). At pH 7.2 the $V_{1/2}$ of common gating for the His847Arg mutant was shifted to more positive potentials, relative to wt, but this shift could not be attributed to the positive charge of the arginine side-chain, as a similar shift was seen with the His847Ala mutant (Fig. 5B, Table 1). Somewhat surprisingly, a decrease in pH_i to 6.2 shifted the common gating curve for the His847Arg mutant to more negative voltages, while both low and high pH_i (pH 7.9) increased the minimum P_o (Fig. 5C, Table 1), reversing the effects of pH changes in wt ClC-1. These results reiterate the important role of His847 in both ATP and proton modulation of ClC-1 common gating. The His847Arg mutation does not, however, reproduce the effects of a decrease in pH_i on wt channels, thus failing to provide any direct support for our hypothesis of an electrostatic interaction between a protonated His847 and the phosphates of ATP. Conversely, these results do not directly refute our hypothesis as the arginine side-chain is not a perfect mimic of a protonated H847.

Another histidine residue in CBS-2 of ClC-1, His835, has been shown to affect the voltage dependence of common gating when mutated to an arginine (25), and is predicted by our CBS domain model to be on the same face of CBS-2 as His847 but too far from the putative ATP-binding site to directly interact with bound ATP (24). To test whether this histidine residue also contributes to pH or ATP modulation of common gating, we measured the effect of pH_i and ATP on a His835Ala mutant. The His835Ala mutation shifted the $V_{1/2}$ of common gating at pH 7.2 by +43 ± 4 mV (Fig. 6, Table 1). This result contrasts with a previous report that a His835Ala mutation had no significant effect on the $V_{1/2}$ of overall channel gating, whilst a His835Arg mutation shifted $V_{1/2}$ by approximately 60 mV (25). The explanation for this discrepancy is not clear but it may be due to the use of different expression systems. We found that common gating of the His835Ala mutant was unaffected by a decrease in pH_i from 7.2 to 6.2 (Fig. 6B, Table 1), indicating that His835 makes a significant contribution to the effect of acidosis on common gating in wt ClC-1. The voltage dependence of common gating for the His835Ala mutant at pH_i 7.9 was similar to that for wt ClC-1 but, because of the shift in $V_{1/2}$ at pH 7.2 due to the His835Ala mutation, the effect of an increase in pH_i from 7.2 to 7.9 is reversed in the His835Ala mutant, relative to wt. Despite the effects of the His835Ala mutation on pH_i modulation of common gating, it had essentially no effect on ATP modulation (Fig. 6B, Table 1). At pH 7.2, 1mM ATP shifted the $V_{1/2}$ of common gating in the His835Ala mutant by +25 ± 3 mV, which is not significantly different to wt. As for wt (Fig. 4), acidosis to pH_i 6.2 markedly enhanced the effect of 1mM ATP on common gating in the His835Ala mutant, shifting the voltage dependence to the point that it does not show saturation by +100 mV (Fig. 6B, best fit of Boltzmann gives $V_{1/2}$ of +67 mV). Finally, a limited dose response curve for ATP suggests that at pH_i 6.2, the His835Ala mutation does not affect the ATP sensitivity of common gating (Fig. 6C). Mutation of a nearby residue S651A, in the cleft between the two CBS domains, had no significant effect on ClC-1 gating or modulation by either ATP (24) or pH (data not shown), supporting the specificity of the mutant effects described above.

Taken together these data demonstrate firstly that at least two protonatable residues, His847 and His835, are important in the effect of intracellular acidosis on ClC-1 common gating. Secondly, they show that the His835Ala mutation separates the independent and ATP-potentiating effects of acidosis, abolishing the effect of acidosis alone whilst retaining ATP-potentiating effect. Thus, the enhanced effect of ATP with acidosis is due primarily to a mechanism other than allosteric cooperativity between the independent effects of ATP and protons. His847 is clearly important for the independent effects of both protons and ATP and may also be important for the cooperative interactions between the two.

Kinetic mechanism of proton and ATP modulation of common gating- To further investigate the mechanism by which intracellular protons and ATP modulate ClC-1 gating, we determined the effect of these ligands on the apparent opening (α) and closing (β) rate constants of the common gate. To calculate these rates, time constants were fitted to the time course of current activation, between 0 and 100 mV, and deactivation, between –140 and –40 mV (Fig. 7A). Deactivating currents were well fit with two exponential components, with the slower of these assumed to correspond to common

gating. For activating currents at positive voltages, this should reduce to a single exponential as protopore gating should be too fast to resolve in macroscopic current activation (14) but there was some indication of a second slow exponential component that may represent a third gating process or multiple closed states of the common gate (23,29). As the two components could not be assigned to particular gating transitions, the analysis was simplified by fitting the time course with a single exponential, assumed to represent the common gate (23). The apparent opening (α) and closing (β) rate constants were calculated from the time constants for current deactivation and activation (τ) and the open probability P_o using equations 4a and b (28).

At pH 7.2, in the absence of ATP, the common gate opening rate constant (α) shows a biphasic dependence on voltage (Fig. 7B), with a positive voltage dependence at positive voltages that reverses to a negative voltage dependence at very negative voltages, whilst the closing rate constant (β) showed a monotonic negative voltage dependence over the entire voltage range tested (Fig. 7C), similar to previous reports for protopore gating of ClC-0 (34) and more recently, for common gating of ClC-1 (23,35). At very negative voltages, the voltage dependence of the opening and closing rates were similar, explaining the voltage-independence and non-zero minimum observed for the open probability at these voltages (23,34).

The biphasic voltage dependence of the opening rate indicates two separate transitions affecting opening that have opposite voltage dependence and hence dominate at opposite extremes of voltage. Chen and Miller (1996) proposed a kinetic scheme for ClC-0 protopore gating (Fig. 8) that accounts for such opposing opening transitions. In this scheme, bound Cl^- acts as the gating charge for the depolarisation-dependent transition (γ) to account the chloride-dependence of gating (34). Although we have not tested chloride-dependence here, others have shown recently that the opening rate of ClC-1 common gating has a similar chloride-dependence to that of ClC-0 protopore gating (35), suggesting that the kinetic scheme of Chen and Miller (1996) also provides a good description for many characteristics of ClC-1 common gating. Consequently we will use this model to investigate the mechanism behind our results, but as all of our experiments were performed at high external [Cl^-] of 152 mM, well above the Cl^- equilibrium constant of 17 mM for ClC-1 common gating (35), we can ignore the portion of this scheme without chloride bound (in grey text, Fig. 8). As the Cl^- gating charge moves through the open channel, gating via this scheme is an inherently non-equilibrium process, leading to great difficulties in assigning closing rate data to particular transitions (34).

At pH 7.2, the primary effect of ATP on the common gating rate constants is to reduce the apparent opening rate (α) relatively uniformly across the whole voltage range (Fig. 7B) with essentially no effect on the closing rate (β) (Fig. 7C). Although ATP appears to have some effect on the voltage-dependence (slope) of the opening rate curves and the relative weighting of the two components, these effects are minor relative to the overall shift to lower rates. In the absence of ATP, an increase in [H^+] from pH 7.2 to 6.2 had a similar effect to ATP on the opening rate, although of slightly smaller magnitude, with again no significant effect on the closing rate (Fig. 7C). These data indicate that in the context of the gating scheme in Scheme I, the independent effects of either ATP or protons can be largely explained by each ligand binding with higher affinity to the closed state C_0 relative to other states (in grey box, Scheme I), stabilising and shifting the equilibrium towards this state. If we then examine the effect on the opening rate of increased [H^+] and ATP together, it is clear that the curve at pH 6.2 plus 1 mM ATP is shifted largely uniformly to lower opening rates in a manner that is essentially additive of the effects of protons and ATP alone, consistent with each ligand acting independently, but this is insufficient to explain the greatly enhanced shift in $V_{1/2}$ due to the synergistic action of [H^+] and ATP together.

The monotonic voltage dependence of the closing rate at pH 7.2 is essentially unaffected by a shift to pH 6.2 or addition of ATP (Fig. 7C), but ATP and acidosis together result in an unusual biphasic voltage dependence, such that the closing rate is markedly increased at positive voltages, becoming almost voltage-independent. The closing rate β is calculated as $\beta = (1 - P_o)/\tau$, but there was no significant difference in the effect on τ of acidosis and ATP together versus either of these factors alone (data not shown). Consequently, the

differential effect of acidosis and ATP together on the voltage dependence of the closing rate is entirely due to their effect on P_o and suffers from the errors in P_o measurements from incomplete curves due to voltage limitations. Hence, we can conclude that the individual inhibitory effects of protons and ATP on common gating are due to stabilisation of the closed state but that the synergistic effects of protons and ATP together appears to involve an extra mechanism that affects the voltage dependence of the closing rate. The practical experimental limits on the voltage range of our measurements preclude a more precise characterization of this extra mechanism.

DISCUSSION

Skeletal muscle acidosis has long been known to lead to a decreased sarcolemmal chloride conductance and more recently this effect has been shown to increase or maintain the excitability of partially depolarised sarcolemma, a mechanism that opposes fatigue. In apparent contradiction to these findings, the activity of ClC-1, the chloride channel responsible for the great majority of sarcolemmal chloride conductance, has been found to be increased by acidosis in recombinant expression systems. The results presented here show a slight inhibition of recombinant ClC-1 by intracellular acidosis, due to a shift in the voltage dependence of common gating to more positive potentials, but more significantly this effect is much greater in the presence of physiological concentrations of ATP. These findings reveal intracellular ATP concentrations as an important factor in the modulation of ClC-1 by acidosis. When this is taken into account, it reveals a significant inhibitory effect of acidosis on recombinant ClC-1 that is consistent with, and provides a rational explanation for, the inhibitory effect of acidosis on skeletal muscle sarcolemmal chloride conductance. The resting intracellular pH of mammalian skeletal muscle is approximately 7.0 but may fall as low as 6.2-6.4 during intense activity (36-40) and recovers over a time-course of approximately 20-25 minutes (41-43). In our experiments, with 5 mM ATP, the normal level in resting or moderately exercising muscle, a reduction of pH_i of this magnitude markedly shifted the voltage dependence of ClC-1 common gating to more positive potentials, inhibiting ClC-1 activity by reducing its open probability across the physiological voltage range. Inhibition of ClC-1 by low intracellular pH in the presence of ATP is therefore likely to be the molecular mechanism underlying the reduction in sarcolemmal chloride-conductance with acidosis that leads to increased membrane excitability (10,11).

During rest and moderate intensity exercise, a variety of homeostatic metabolic systems maintain ATP levels in skeletal muscle cells at close to 5 mM but during very intense exercise, ATP can be depleted in fast-twitch fibre types, where ClC-1 expression is highest (44), to less than 25% of resting levels within 25 s of intense activity (45). In the absence of any acidosis, this degree of ATP depletion would significantly relieve ATP inhibition of ClC-1, effectively activating ClC-1 and leading us to propose that this may reduce muscle excitability and contribute to fatigue whilst protecting muscles from metabolic exhaustion (24). Our current results show that acidosis, which would occur with any muscle activity sufficiently intense to deplete ATP levels, markedly increases the $\Delta V_{1/2}$ caused by all concentrations ATP and also appears to increase the apparent affinity for ATP. Even without any affinity change the enhanced $\Delta V_{1/2}$ with acidosis, particularly for low ATP concentration, brings into question whether ATP depletion would ever return the $V_{1/2}$ to sufficiently negative potentials for the resulting activation of ClC-1 to play a physiologically significant role in contributing to fatigue. Such questions can only be answered when the combined effects of acidosis, ATP depletion and membrane depolarisation on membrane excitability are all considered in the context of active skeletal muscle tissue. Certainly, when the synergistic effects of acidosis and ATP on ClC-1 are taken into account, it appears likely that any reduction in excitability due to ATP depletion would occur via modulation of K_{ATP} channels (46) and ryanodine receptors (47) before any effect via modulation of ClC-1.

Although the shift in the $V_{1/2}$ of common gating to more positive voltages due to acidosis in the presence of ATP is the most physiologically relevant effect presented here, we also found a slight shift in the same direction with acidosis in the absence of ATP, contrary to previous studies which showed that reducing intracellular pH shifts voltage dependence, marginally, to more negative

potentials (14,29). One possible explanation for this discrepancy is the length of the conditioning pulse. Our results with shorter conditioning voltage-pulses are consistent with earlier studies also employing short voltage pulses; that is, at pH 6.2 the voltage dependence of common gating is shifted to more negative potentials with respect to pH 7.2. When we used longer pulses to allow for the slowed current kinetics at low pH, however, the voltage dependence of common gating was shifted to more positive potentials. Another possible explanation for the positive shift of voltage dependence that we have observed with acidosis may be due to residual intracellular ATP. Because of the increased ATP sensitivity at low pH, even small amounts of ATP remaining in the cell after 5 or more minutes of dialysis against the ATP-free pipette solution would be expected to shift common gating to more positive potentials. Although experiments performed by Rychkov and co-authors were also in whole-cell configuration, they studied the rat isoform o f ClC-1 expressed in Sf9 insect cells, where ATP regulation of ClC-1 may be different (15,29). Accardi and Pusch studied ClC-1 pH sensitivity in inside-out membrane patches taken from *Xenopus* oocytes, where no ATP was present (14). Obviously more experiments are required to clarify whether the small positive shift in the voltage dependence of common gating that we observed at low pH is a direct effect of protonation of the channel or is due to low level binding of residual ATP.

We propose, based on mutational analysis and molecular modelling, presented previously (24) and further developed here, that the effects of ATP on ClC-1 gating are due to direct binding of ATP to the C-terminal CBS domains of ClC-1. We now propose further, again based on mutational analysis presented here, that the modulation of ClC-1 gating by intracellular pH is due to direct protonation of histidine residues in the CBS domains and interaction of these residues with ATP binding. We cannot entirely rule out that these modulatory effects are mediated indirectly by other components of the intracellular milieu but the mutational evidence, the interaction between ATP and pH modulation and the structural resolution of nucleotide-binding sites in CBS domains combine to strongly favour direct modulation for both ATP and protons.

Base on our molecular modelling, together with three experimental findings presented here; the apparent pK_a for the pH sensitivity of ClC-1 common gating being compatible with the protonation of histidine residues, the increased effect of ATP with acidosis and the lack of any increased effect of adenosine, which lacks phosphate groups, we hypothesized that the increased apparent affinity for ATP may be due to electrostatic interactions between protonated His847 and the phosphates of ATP. Consistent with this hypothesis, as well as abolishing the effect of ATP at pH 7.2 (24), mutations of His847 also abolished the effect of acidosis in the absence of ATP, and greatly attenuated the effect of ATP and acidosis together. We have not been able to provide any more direct support for this hypothesis as our attempt to mimic protonation of His847 with a His847Arg mutation failed to produce the same effect as acidosis. Interestingly, the ClC-5 residue equivalent to His847 is an arginine and although in reasonable proximity to the phosphates of bound ATP, it was not found to interact closely with these groups in the crystal structure (31).
Mutation of His835, that has been shown to affect ClC-1 gating (25), was also found here to abolish the effect of acidosis on common gating, in the absence of ATP, but had essentially no effect on ATP modulation at pH 7.2 and only slightly reduced the enhanced effect of ATP with acidosis. The lack of effect of the His835Ala mutation on ATP modulation is consistent with its location in our model, approximately 20 Å from His847 and the putative ATP-binding site. Conversely, the similar effects of His835Ala and His847Ala mutations, in abolishing direct acidosis modulation of common gating, may be explained by these residues being on the same face of the CBS domain model, a face that may be important for modulation of gating by affecting CBS domain dimerisation or interaction with the channel domain. Collectively these results demonstrate that mutations can separate the direct effect of acidosis, in the absence of ATP, and the potentiating effect of acidosis on ATP modulation, with both His835 and His847 contributing to the direct effect of acidosis but only His847 being important for the ATP potentiating effect. These results are consistent with our hypothesis of an electrostatic interaction between the phosphates of ATP and protonated His847 but, given that mutations of His847 also abolish direct effects of ATP, we remain without any direct evidence that this

interaction occurs and is responsible for the synergistic effects of acidosis and pH in inhibiting ClC-1.

To understand the underlying mechanism of pH and ATP modulation of ClC-1 common gating, we measured the effect of pH and ATP on kinetic parameters of gating relaxation and gating rate constants, ion the context of a simple two state model. From this analysis, we could conclude that the individual inhibitory effects of protons and of ATP on common gating were due to stabilisation of the closed state. The synergistic effects of protons and ATP together appeared to involve an extra mechanism affecting the voltage dependence of the closing rate. Practical experimental limits on the voltage range of our measurements precluded both a more precise characterization of this extra mechanism and any more detailed analysis of the underlying kinetics.

In summary, we have demonstrated that low intracellular pH and ATP act synergistically to inhibit ClC-1 chloride channels by shifting the voltage dependence of common gating to more positive potentials. Modulation of ClC-1 gating by pH_i and ATP is therefore likely to be the molecular mechanism that underlies increased excitability in acidified skeletal muscle. The kinetics of these modulatory effects indicates that ATP and protons act independently by stabilising the closed state of the common gate but also act cooperatively via a separate mechanism that involves alteration of the voltage dependence of the closing rate. His847 in the carboxy-terminal CBS domains of ClC-1 is a critical residue for the effects of both protons and ATP, consistent with our hypothesis that it contributes directly to a putative ATP-binding site. Further structural characterisation will be required to determine the veracity of this hypothesis.

REFERENCES

1. Ruff, R. L. (1996) *Acta Physiol Scand* **156**(3), 159-168
2. Sejersted, O. M., and Sjogaard, G. (2000) *Physiol Rev* **80**(4), 1411-1481
3. Bretag, A. H. (1987) *Physiol Rev* **67**(2), 618-724
4. Steinmeyer, K., Ortland, C., and Jentsch, T. J. (1991) *Nature* **354**(6351), 301-304.
5. Chen, M. F., Niggeweg, R., Iaizzo, P. A., Lehmann-Horn, F., and Jockusch, H. (1997) *J Physiol* **504**(Pt 1), 75-81.
6. Koch, M. C., Steinmeyer, K., Lorenz, C., Ricker, K., Wolf, F., Otto, M., Zoll, B., Lehmann-Horn, F., Grzeschik, K. H., and Jentsch, T. J. (1992) *Science* **257**(5071), 797-800.
7. Pusch, M. (2002) *Hum Mutat* **19**(4), 423-434.
8. Fitts, R. H. (1994) *Physiol Rev* **74**(1), 49-94
9. Nielsen, O. B., de Paoli, F., and Overgaard, K. (2001) *J Physiol* **536**(Pt 1), 161-166
10. Pedersen, T. H., de Paoli, F., and Nielsen, O. B. (2005) *J Gen Physiol* **125**(2), 237-246
11. Pedersen, T. H., Nielsen, O. B., Lamb, G. D., and Stephenson, D. G. (2004) *Science* **305**(5687), 1144-1147
12. Hutter, O. F., and Warner, A. E. (1967) *J Physiol* **189**(3), 403-425
13. Palade, P. T., and Barchi, R. L. (1977) *J Gen Physiol* **69**(3), 325-342
14. Accardi, A., and Pusch, M. (2000) *J Gen Physiol* **116**(3), 433-444.
15. Rychkov, G. Y., Pusch, M., Roberts, M. L., and Bretag, A. H. (2001) *J Physiol* **530**(Pt 3), 379-393.
16. Rychkov, G. Y., Pusch, M., Roberts, M. L., Jentsch, T. J., and Bretag, A. H. (1998) *J Gen Physiol* **111**(5), 653-665.
17. Middleton, R. E., Pheasant, D. J., and Miller, C. (1996) *Nature* **383**(6598), 337-340
18. Dutzler, R., Campbell, E. B., Cadene, M., Chait, B. T., and MacKinnon, R. (2002) *Nature* **415**(6869), 287-294.
19. Saviane, C., Conti, F., and Pusch, M. (1999) *J Gen Physiol* **113**(3), 457-468.

20. Dutzler, R., Campbell, E. B., and MacKinnon, R. (2003) *Science* **300**(5616), 108-112.
21. Bennetts, B., Roberts, M. L., Bretag, A. H., and Rychkov, G. Y. (2001) *J Physiol* **535**(Pt 1), 83-93.
22. Pusch, M., Ludewig, U., and Jentsch, T. J. (1997) *J Gen Physiol* **109**(1), 105-116
23. Duffield, M., Rychkov, G., Bretag, A., and Roberts, M. (2003) *J Gen Physiol* **121**(2), 149-161.
24. Bennetts, B., Rychkov, G. Y., Ng, H. L., Morton, C. J., Stapleton, D., Parker, M. W., and Cromer, B. A. (2005) *J Biol Chem* **280**, 32452-32458
25. Estevez, R., Pusch, M., Ferrer-Costa, C., Orozco, M., and Jentsch, T. J. (2004) *J Physiol*
26. Aromataris, E. C., Rychkov, G. Y., Bennetts, B., Hughes, B. P., Bretag, A. H., and Roberts, M. L. (2001) *Mol Pharmacol* **60**(1), 200-208.
27. Barry, P. H. (1994) *J Neurosci Methods* **51**(1), 107-116
28. Chen, T. Y. (1998) *J Gen Physiol* **112**(6), 715-726.
29. Rychkov, G. Y., Pusch, M., Astill, D. S., Roberts, M. L., Jentsch, T. J., and Bretag, A. H. (1996) *J Physiol* **497**(Pt 2), 423-435.
30. Corfu, N. A., and Sigel, H. (1991) *Eur J Biochem* **199**(3), 659-669
31. Meyer, S., and Dutzler, R. (2006) *Structure* **14**(2), 299-307
32. Meyer, S., Savaresi, S., Forster, I. C., and Dutzler, R. (2007) *Nat Struct Mol Biol* **14**(1), 60-67
33. Townley, R., and Shapiro, L. (2007) *Science* **315**(5819), 1726-1729
34. Chen, T. Y., and Miller, C. (1996) *J Gen Physiol* **108**(4), 237-250
35. Hebeisen, S., and Fahlke, C. (2005) *Biophys J* **89**(3), 1710-1720
36. Hermansen, L., and Osnes, J. B. (1972) *J Appl Physiol* **32**(3), 304-308
37. Metzger, J. M., and Fitts, R. H. (1987) *J Appl Physiol* **62**(4), 1392-1397
38. Roos, A., and Boron, W. F. (1978) *Am J Physiol* **235**(1), C49-54
39. Sahlin, K., Alvestrand, A., Brandt, R., and Hultman, E. (1978) *J Appl Physiol* **45**(3), 474-480
40. Wilson, J. R., McCully, K. K., Mancini, D. M., Boden, B., and Chance, B. (1988) *J Appl Physiol* **64**(6), 2333-2339
41. Metzger, J. M., Greaser, M. L., and Moss, R. L. (1989) *J Gen Physiol* **93**(5), 855-883
42. Sahlin, K., Harris, R. C., Nylind, B., and Hultman, E. (1976) *Pflugers Arch* **367**(2), 143-149
43. Thompson, L. V., Balog, E. M., and Fitts, R. H. (1992) *Am J Physiol* **262**(6 Pt 1), C1507-1512
44. Papponen, H., Kaisto, T., Myllyla, V. V., Myllyla, R., and Metsikko, K. (2005) *Exp Neurol* **191**(1), 163-173
45. Karatzaferi, C., de Haan, A., Ferguson, R. A., van Mechelen, W., and Sargeant, A. J. (2001) *Pflugers Arch* **442**(3), 467-474
46. Noma, A. (1983) *Nature* **305**(5930), 147-148
47. Dutka, T. L., and Lamb, G. D. (2004) *J Physiol* **560**(Pt 2), 451-468
48. DeLano, W.L. The PyMOL Molecular Graphics System (2002) http://www.pymol.org

FOOTNOTES

This work was supported by a grant from the National Health and Medical Research Council of Australia (NHMRC) to M.W.P. and B.A.C.. M.W.P. is an Australian Research Council Federation Fellow. We thank Dr. Grigori Y. Rychkov, Prof. Graham Lamb and Dr. Steven Petrou for constructive comments and advice on this work.

FIGURE LEGENDS

Fig. 1. Dependence of ClC-1 common-gating open probability on voltage-pulse length at low intracellular pH. (A) Voltage protocol with a test pulse of 100-800 ms, stepped from -140 to 100 mV in successive sweeps followed by a 75 ms tail pulse at a set -100 mV. To measure the common gate only, a brief (400 μs) pulse to +170 mV (dotted line) is added at the end of the conditioning pulse, just before the tail pulse, to fully activate the protopore gates, as detailed in the method section. Capacitative currents have been blanked on this figure. Time scale in panel B applies to panels A and B. (B) Representative current traces from HEK 293 cells expressing ClC-1 at intracellular pH 6.2, with different length conditioning voltage pulses. (C) Open probability of the common gate with different pulse lengths, calculated from the current traces in A. Solid lines represent fits of eq. 2 to the data points, with $V_{1/2}$ values (100 ms) –110 mV, (200 ms) –85 mV, (400 ms) –57 mV and (800 ms) –48 mV.

Fig. 2. Dependence of ClC-1 gating on intracellular pH in the absence of ATP. (A) Representative current traces recorded at different intracellular pH. Broken lines indicate zero-current level. Capacitative currents have been blanked on this figure. (B) pH dependence of apparent channel open probability. (C) pH dependence of common gating. (D) pH dependence of fast gating. Solid lines in B, C and D represent fits of eq. 2 to the experimental data points.

Fig. 3. Effect of intracellular pH and ATP, or adenosine, on ClC-1 common gating. (A) Representative current trace from ClC-1 at low intracellular pH with ATP. Dotted line indicates zero-current level. Capacitative transients have been blanked on this figure. (B) Common gating curves for ClC-1 at pH 7.2 (○), pH 7.2 + 1 mM ATP (●), pH 6.2 (Δ), pH 6.2 + 1 mM ATP (▲). Data points are means ± S.E.M determined from 3-5 cells. Solid lines represent fits of eq. 2 to the experimental data. (C) Effect of intracellular ligands Mg-ATP (filled symbols) on the $V_{1/2}$ of the channel overall at pH 6.2 (▼) and of the common gate at pH 6.2 (▲) or pH 7.2 (●). Open symbols show the effect of adenosine on $V_{1/2}$ at pH 6.2 (Δ) or pH 7.2 (○). Data for Mg-ATP at pH 7.2 and for adenosine are plotted against the right ordinate-axis only. Lines represent the fit of Michaelis-Menten type functions to the Mg-ATP data sets. (D) pH dependence of ATP effect on common gating. Intracellular pH was varied at constant 1 mM ATP. Solid line represents a fit of a sigmoidal curve to the experimental data points. Open probability data at pH 6.2 with high ATP concentrations do not reach a plateau in the measured voltage range (B). Consequently, error bars in panels C and D for points derived from these data are estimates of the range of $V_{1/2}$ values to which the data can be fit and maintain $R^2 > 0.9995$. Arrows at the top end of the error bar indicate that higher $V_{1/2}$ values also fit the data but only with markedly increasing slope values (k in equation 2).

Fig. 4. Model of CBS domains of ClC-1 built by homology to CBS domains of ClC-0, 2D4Z (31). Shown as bonds are two feasible binding poses of AMP, identified by computational docking, that correspond closely either with docking to our earlier model (24) or with nucleotide bound to ClC-5 CBS domains (32). AMP is coloured by atom with ribose carbons of the two poses coloured cyan and magenta, respectively. Panels **A** and **B** show both poses of AMP. Panels **C** and **D** are rotated 90° around the x-axis relative to the upper panels and show only the "new" pose corresponding to that seen in ClC-5. In panels **A** and **C,** the protein is shown as van der Waals surface, coloured by atom, with CBS-1 on the left and CBS-2 on the right. In panels **B** and **D** the protein backbone is shown as a ribbon, coloured blue to red from N- to C- terminus, with sidechains close to AMP labelled and shown as bonds coloured by atom, with carbon coloured yellow. In all panels, His847 and Leu848 are shown in cyan and olive green, respectively. This figure was produced using PyMOL (48).

Fig. 5. Intracellular pH and nucleotide sensitivity of His847 mutants. (A) Representative current traces from cells expressing mutants His847A and His847Arg with internal solution at pH 7.2 with no ATP. Broken lines indicate zero-current level. Capacitative transients have been blanked on this figure. Currents were recorded using a voltage protocol containing a brief pulse to +170 mV to isolate the common gate, detailed in the methods section. (B) $P_o(V)$ of the common gate of mutant His847Ala at pH 7.2 (○), pH 7.9 (◊), pH 6.2 (Δ),pH 7.2 + 5 mM ATP (●) and pH 6.2 + 5 mM ATP (▲). Solid lines represent the fit of eq. 2 to experimental data points. Dotted and dashed lines represent the fit of eq. 2 to

WT data from Fig. 3 C at pH 6.2 and at pH 6.2 + 1 mM ATP, respectively. (C) $P_o(V)$ of the common gate of mutant His847Arg. Symbols and lines are the same as for (B), except all ATP concentrations are 1 mM.

Fig. 6. pH and nucleotide sensitivity of His835Ala mutant. (A) Representative current traces from cells expressing mutant His835Ala with internal solution at pH 7.2 with no ATP. Broken lines indicate zero-current level. Capacitative transients have been blanked on this figure. Currents were recorded using a voltage protocol containing a brief pulse to +170 mV to isolate the common gate, detailed in the methods section. (B) $P_o(V)$ of the common gate of mutant His835Ala at pH 7.2 (○), pH 7.9 (◊), pH 6.2 (Δ), pH 7.2 + 1 mM ATP (●) and pH 6.2 + 1 mM ATP (▲). Solid lines represent the fit of eq. 2 to experimental data points. Dotted and dashed lines represent the fit of eq. 2 to WT data from Fig. 3 C at pH 6.2 and at pH 6.2 + 1 mM ATP, respectively. (C) ATP dependence of WT ClC-1 and His835Ala common gating at pH 6.2. Large error bars shown for very positive values of $V_{1/2}$ represent an estimated range derived from open probability curves that do not reach a clear plateau, as described for Fig. 3 C.

Fig. 7. Current kinetics and apparent rate constants for ClC-1 common gating. (A). Current activation and deactivation from representative cells with intracellular conditions as labelled. Broken lines indicate zero-current level. Capacitative transients have been blanked on this figure. Activation (current traces in the top of panel A) was recorded using 500 ms voltage pulses in 20 mV increments from 0 mV to 100 mV directly after a 200 ms pulse to –140 mV to deactivate current (not shown). Deactivation (current traces in the bottom of panel A) was recorded using 500 ms voltage pulses from –140 mV to –40 mV in 20 mV increments directly after a 200 ms 100 mV pulse to maximally activate current (not shown). Scale is as shown at the bottom right of each family of current traces. (B). Opening rate constants for common gating at pH 7.2 (○), pH 6.2 (Δ), pH 7.2 + 5 mM ATP (●) and pH 6.2 + 1 mM ATP (▲). Solid lines represent fits of a double exponential function to the experimental data points. (C). Closing rate constants for ClC-1 common gating. Symbols are the same as in panel (B). Solid lines represent the fit of single exponential functions to the experimental data points. All data points in panels (B) and (C) are means ± S.E.M.

Fig. 8. Kinetic scheme proposed by Chen and Miller (1996) to explain characteristics of ClC-0 protopore gating but that also appears useful in describing the properties of ClC-1 common gating. The part of the scheme shown in grey text is not significant at the saturating chloride concentrations used in all our experiments. The grey box includes all states that can be grouped together as "Open" in a simplified two-state scheme.

TABLES

		Intracellular solution				
mutant		pH 7.9	pH 7.2	pH 7.2 + ATP 1 (*or 5)* mM	pH 6.2	pH 6.2 + ATP 1 (*or 5)* mM
WT	$V_{1/2}$	-37 ± 2	-70 ± 2	-51 ± 3	-45.2 ± 1.5	+71 ± 25 [a]
	P_{min}	0.41 ± 0.01	0.37 ± 0.01	0.01 ± 0.02	0.11 ± 0.01	0.04 ± 0.01
H847A	$V_{1/2}$	-49.4 ± 0.9	-46.7 ± 1.0	*-41 ± 2*	-40 ± 2	*-21.1 ± 1.5*
	P_{min}	0.40 ± 0.01	0.25 ± 0.01	*0.19 ± 0.01*	0.20 ± 0.01	*0.14 ± 0.01*
H847R	$V_{1/2}$	-59 ± 5	-50.1 ± 1.5	-52.6 ± 0.7	-74 ± 4	-41.7 ± 1.0
	P_{min}	0.50 ± 0.03	0.27 ± 0.01	0.26 ± 0.01	0.37 ± 0.03	0.18 ± 0.01
H835A	$V_{1/2}$	-42 ± 2	-27 ± 2	+2.2 ± 0.9	-27.5 ± 1.3	+67 ± 25 [a]
	P_{min}	0.25 ± 0.02	0.07 ± 0.02	0.03 ± 0.01	0.04 ± 0.01	0.10 ± 0.01

Table 1. Parameters of common-gating curves for wt and mutant ClC-1 with various intracellular solutions. Values of $V_{1/2}$ and P_{min} were determined from fits of eq. 2 to experimental data points. Figures in *italics* are for *5 mM ATP*. [a] $V_{1/2}$ estimates from non-saturating curves with consequently large errors associated.

g. 1

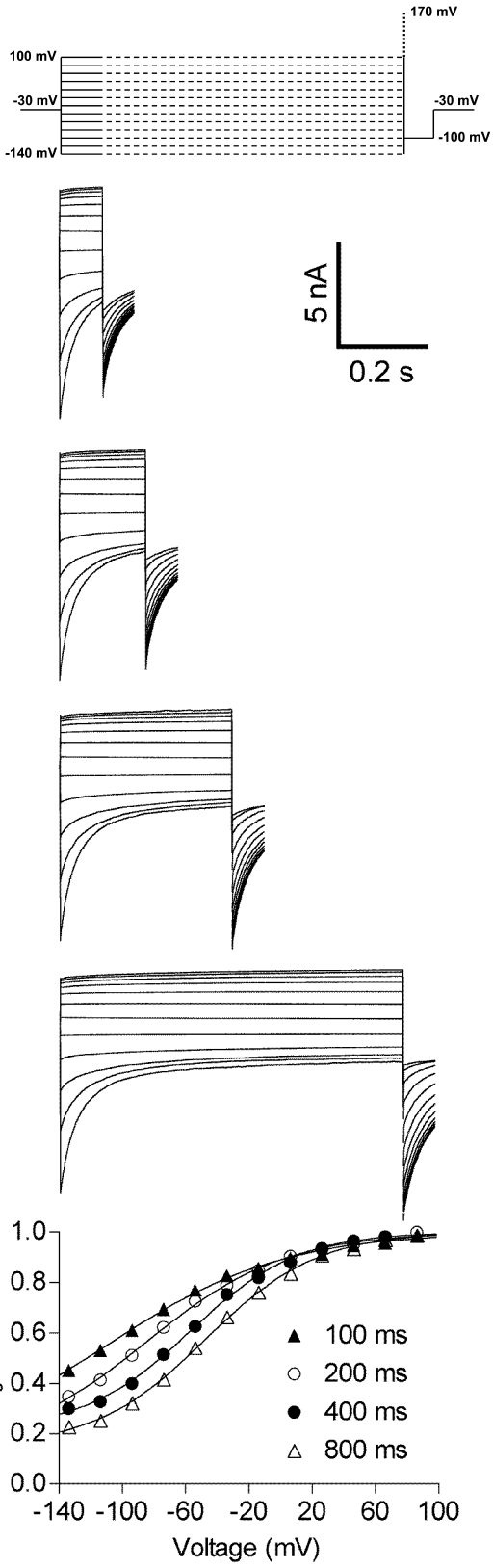

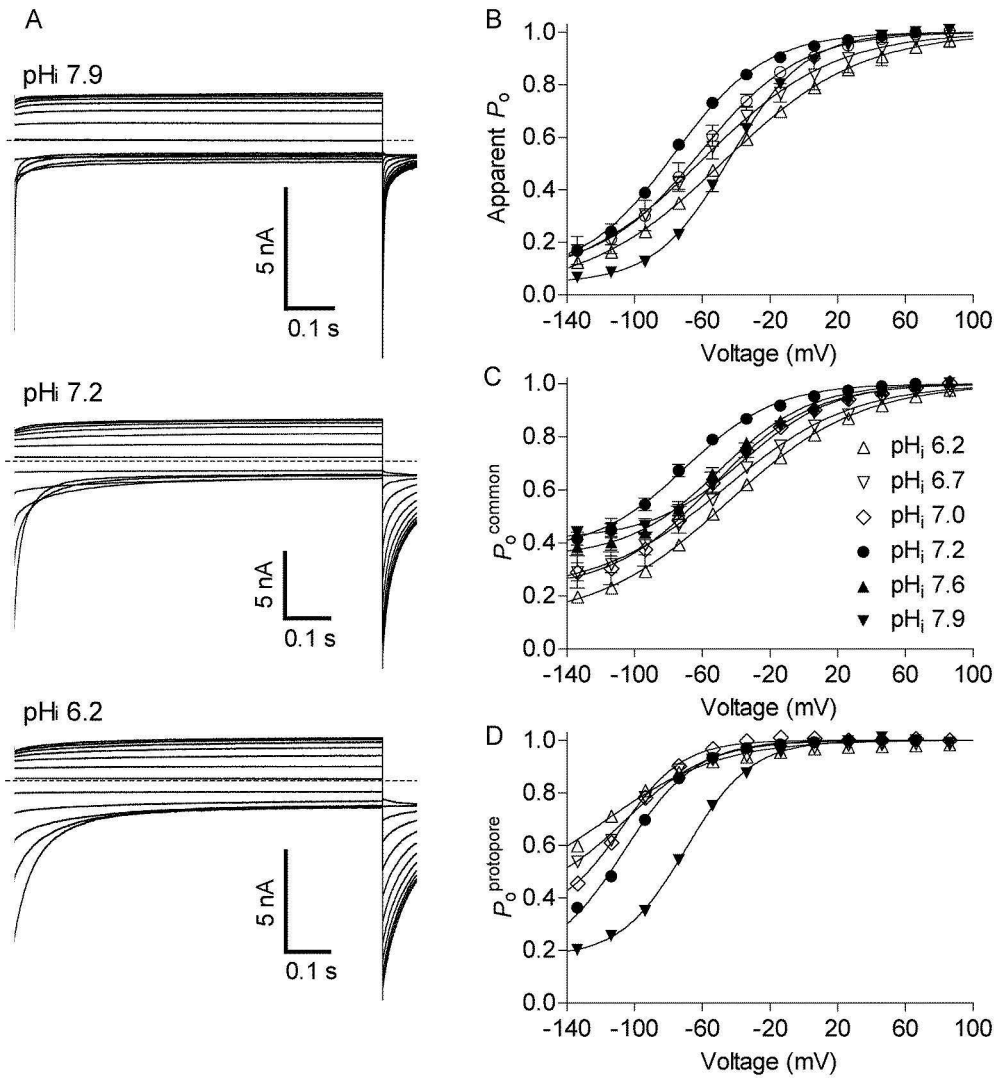

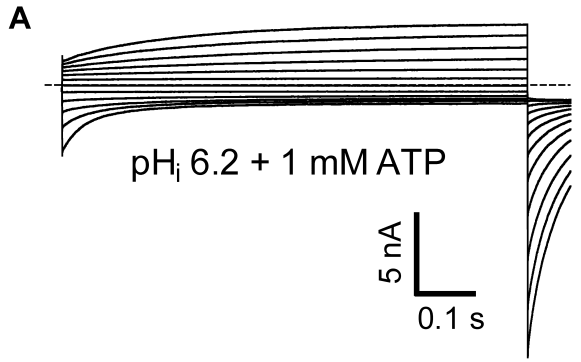
A
pH$_i$ 6.2 + 1 mM ATP
5 nA
0.1 s

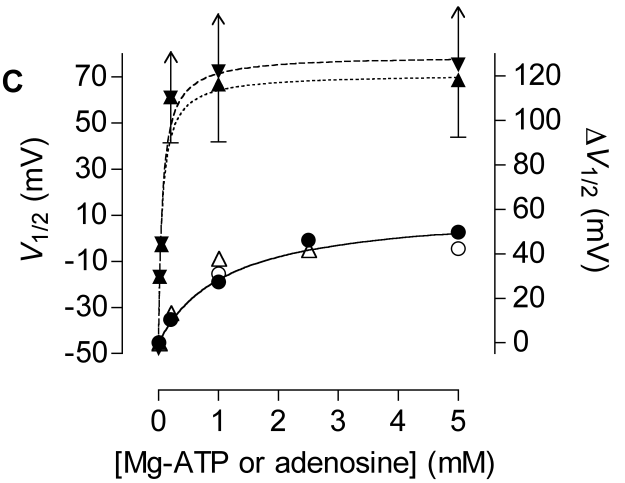
C
$V_{1/2}$ (mV)
$\Delta V_{1/2}$ (mV)
[Mg-ATP or adenosine] (mM)

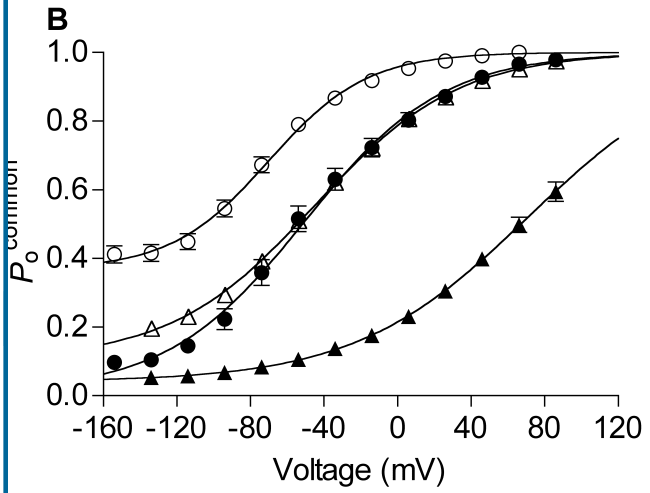
B
P_o^{common}
Voltage (mV)

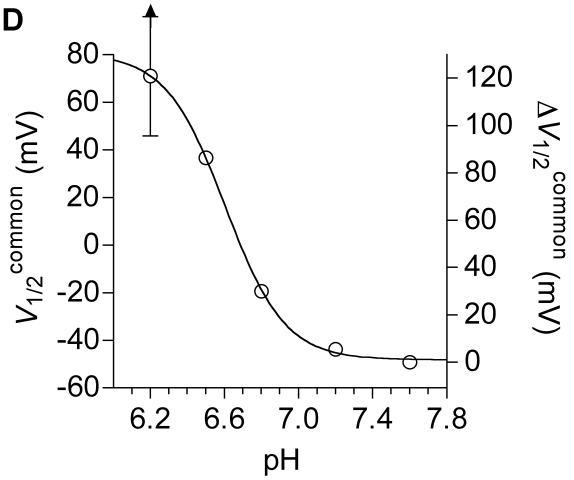
D
$V_{1/2}^{common}$ (mV)
$\Delta V_{1/2}^{common}$ (mV)
pH

.4

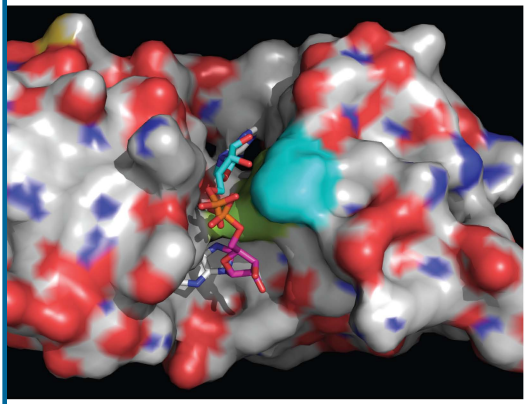

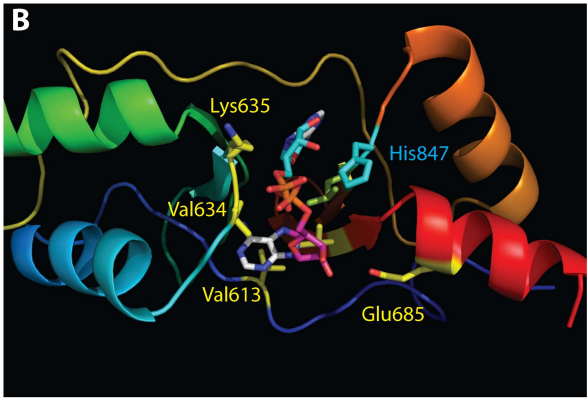
B
Lys635
His847
Val634
Val613
Glu685

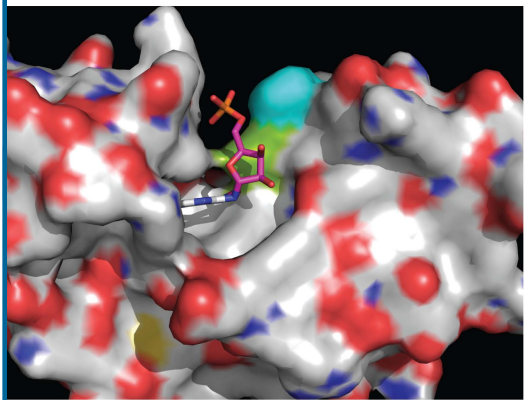

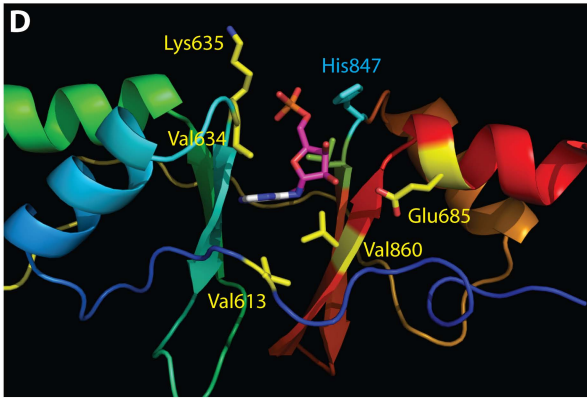
D
Lys635
His847
Val634
Glu685
Val860
Val613

Fig. 5

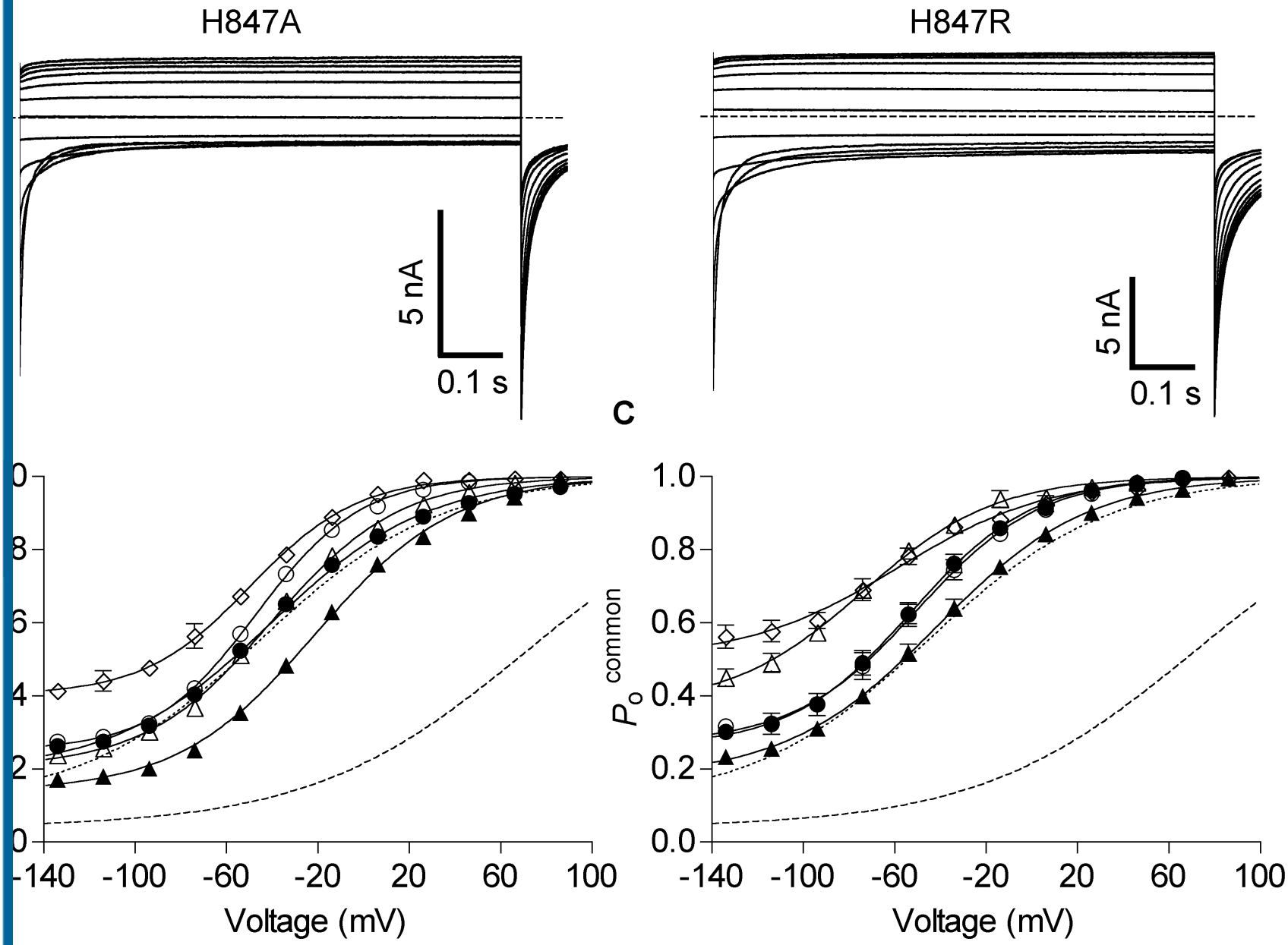
H847A
H847R
5 nA
0.1 s
5 nA
0.1 s
C
1.0
0.8
0.6
0.4
0.2
0.0
P_o common
-140
-100
-60
-20
20
60
100
Voltage (mV)
-140
-100
-60
-20
20
60
100
Voltage (mV)

Fig. 6

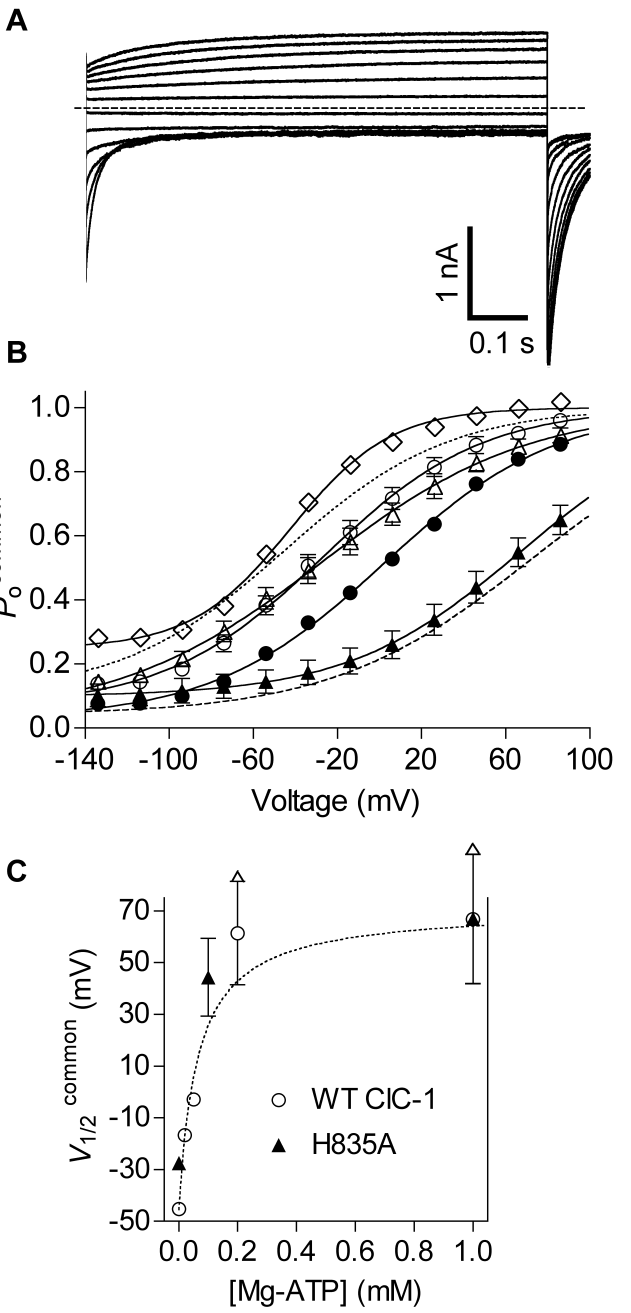

Fig. 7

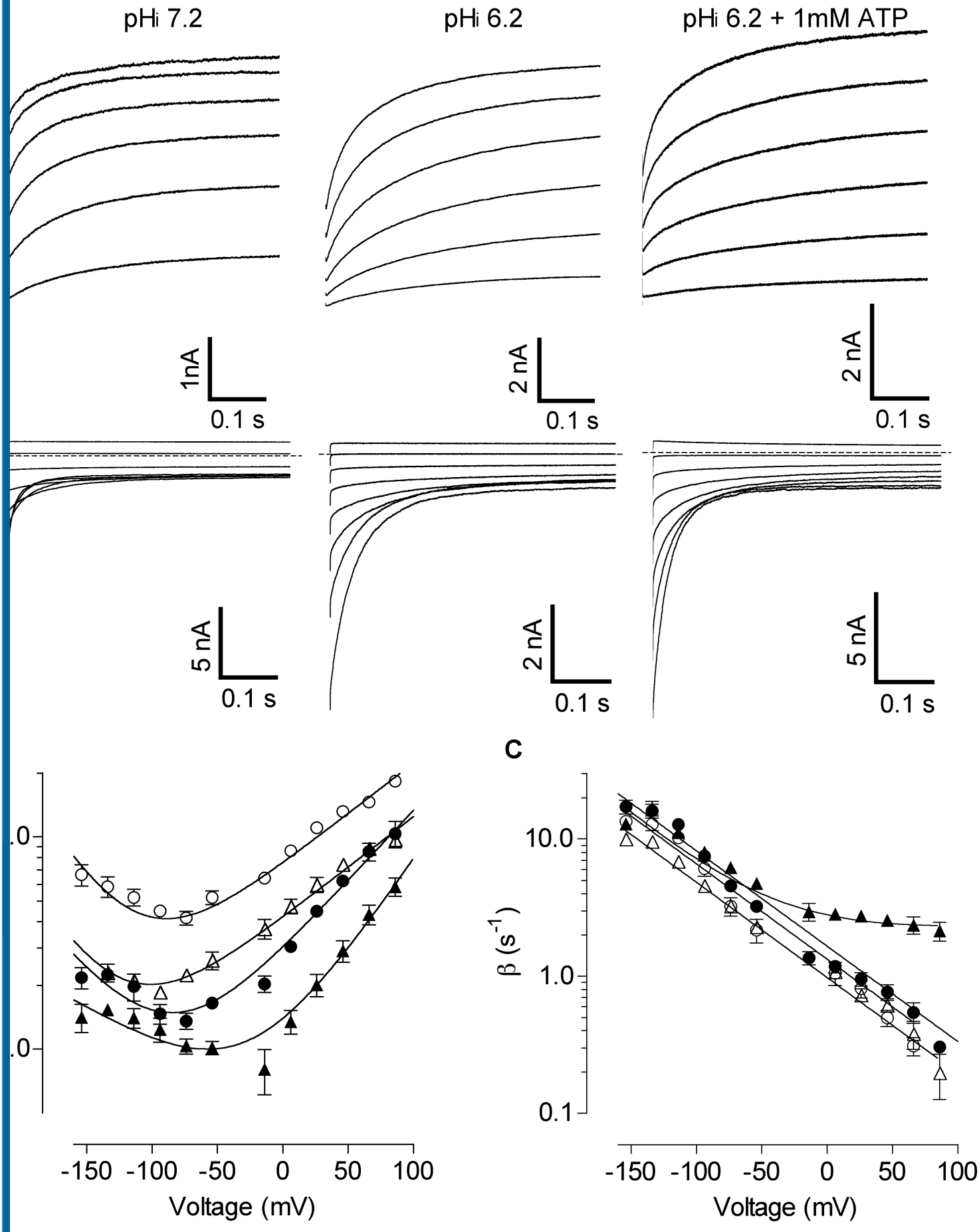
pHi 7.2
pHi 6.2
pHi 6.2 + 1mM ATP
1nA
0.1 s
2 nA
0.1 s
2 nA
0.1 s
5 nA
0.1 s
2 nA
0.1 s
5 nA
0.1 s
C
β (s-1)
10.0
1.0
0.1
-150 -100 -50 0 50 100
Voltage (mV)
-150 -100 -50 0 50 100
Voltage (mV)

g. 8

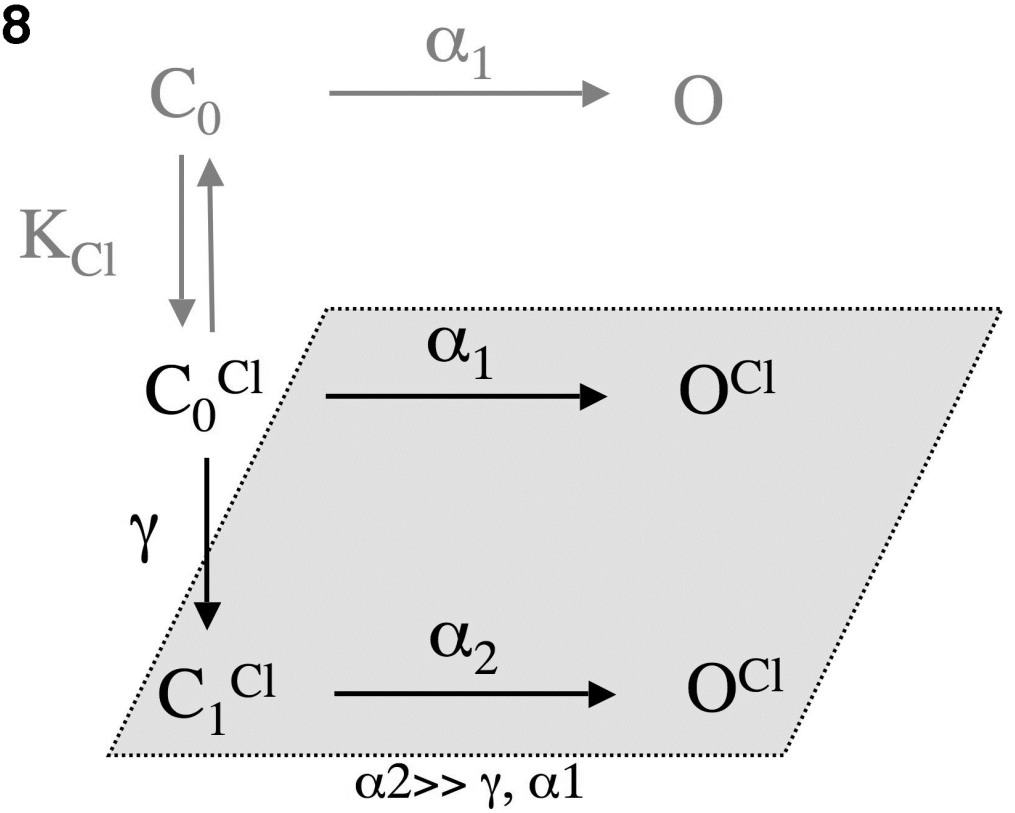
α_1
C_0
O
K_{Cl}
C_0^{Cl}
α_1
O^{Cl}
γ
α_2
C_1^{Cl}
O^{Cl}
$\alpha 2 >> \gamma, \alpha 1$